UC Davis

Title

Gamma-band entrainment abnormalities in schizophrenia: Modality-specific or cortex-wide impairment?

Permalink

Journal

Authors

Erickson, Molly
Lopez-Calderon, Javier
Robinson, Ben
et al.

Publication Date

DOI

Gamma-band entrainment abnormalities in schizophrenia: Modality-specific or cortex-wide impairment?

Molly A. Erickson[1,a], **Javier Lopez-Calderon**[2], **Ben Robinson**[3], **James M. Gold**[3], **Steven J. Luck**[4]

[1]University of Chicago Department of Psychiatry & Behavioral Neuroscience

[2]Centro de Investigaciones Médicas, Escuela de Medicina, Universidad de Talca

[3]Maryland Psychiatric Research Center, University of Maryland

[4]Center for Mind & Brain and Department of Psychology, University of California, Davis

Abstract

Objective.—A growing body of literature suggests that cognitive impairment in people with schizophrenia (PSZ) results from disrupted cortical excitatory/inhibitory (E-I) balance, which may be linked to gamma entrainment and can be measured noninvasively using electroencephalography (EEG). However, it is not yet known the degree to which these entrainment abnormalities covary within subjects across sensory modalities. Furthermore, the degree to which cross-modal gamma entrainment reflects variation in biological processes associated with cognitive performance remains unclear.

Methods.—We used EEG to measure entrainment to repetitive auditory and visual stimulation at beta (20 Hz) and gamma (30 and 40 Hz) frequencies in PSZ (n=78) and healthy control subjects (HCS; n=80). Three indices were measured for each frequency and modality: event-related spectral perturbation (ERSP), inter-trial coherence (ITC), and phase-lag angle (PLA). Cognition and symptom severity were also assessed.

Results.—We found little evidence that gamma entrainment covaried across sensory modalities. PSZ exhibited a modest correlation between modalities at 40 Hz for ERSP and ITC measures (r=0.26-0.27); however, no other significant correlations between modalities emerged for either HCS or PSZ. Both univariate and multivariate analyses revealed that (a) the pattern of entrainment abnormalities in PSZ differed across modalities, and (b) modality rather than frequency band was the main source of variance. Finally, we observed a significant association between cognition and gamma entrainment in the auditory domain only in HCS.

Conclusions.—Gamma-band EEG entrainment does not reflect a unitary transcortical mechanism but is instead modality specific. To the extent that entrainment reflects the integrity

of cortical E-I balance, the deficits observed in PSZ appear to be modality specific and not consistently associated with cognitive impairment.

General Scientific Summary

This study suggests that gamma entrainment abnormalities in people with schizophrenia, which are commonly thought to reflect impairment in excitatory and inhibitory neurotransmitter signaling in the cortex, are not consistently observed across sensory modalities. Furthermore, gamma entrainment abnormalities are not associated with cognitive impairment in patients.

Keywords

schizophrenia; entrainment; gamma; EEG; cognition

Introduction

People with schizophrenia (PSZ) typically exhibit a broad spectrum of cognitive impairment, which is unlike the effects of focal brain damage. This broad spectrum might instead reflect impaired microcircuit integrity, and interest in this hypothesis has grown considerably over the past decade (see Smucny et al., 2021 for a recent review). Much of the evidence for microcircuit disruption in PSZ is drawn from postmortem investigations revealing a disturbance in fast-spiking, parvalbumin-expressing (PV+) interneurons within a variety of brain regions such as the prefrontal cortex (Bitanihirwe & Woo, 2014; Chung et al., 2016; see Kaar et al., 2019 for a meta-analysis; Reynolds et al., 2002), hippocampus (Knable et al., 2004; Konradi et al., 2011; Zhang & Reynolds, 2002), parahippocampus (A. Y. Wang et al., 2011), entorhinal cortex (Reynolds et al., 2002), orbitofrontal cortex (Joshi et al., 2015), and visual and posterior parietal cortices (Fish et al., 2021). PV+ interneuron disruption has even been observed in subcortical structures such as the inferior colliculus (Kilonzo et al., 2020) and thalamus (Danos et al., 1998).

Although early reports of this phenomenon implicated reduced neuronal density as the primary source of disruption in PSZ, more recent work indicates that the loss of inhibitory function appears to also emerge from decreased excitatory synapse density on the PV+ interneurons even when they are present in numbers comparable to those in healthy control subjects (HCS; Chung et al., 2016). This widespread weakening of inhibition in PSZ is thought to reflect a compensatory response to abnormally low pyramidal excitation, thereby restoring excitatory/inhibitory (E-I) balance within the cortex; the result of these homeostatic changes is that the cortex has neither the excitatory nor inhibitory strength to produce gamma oscillations necessary to meet cognitive demands (for reviews see Gonzalez-Burgos et al., 2015; Lewis et al., 2012).

Cortical gamma oscillations, which are measured using electroencephalography (EEG) and magnetoencephalography (MEG), typically range from 30-100 Hz and appear to emerge from dynamic interactions between PV+ interneurons and pyramidal cells within cortical columns (Bartos et al., 2007; Sohal et al., 2009). The magnitude and coherence of the gamma oscillation are therefore considered useful *in vivo* proxy measures of cortical E-I integrity both in humans (Cardin, 2016; Gonzalez-Burgos et al., 2015) and in animal models

of schizophrenia (e.g., Bartley et al., 2015; Cunningham et al., 2006; Dricks, 2016; Fisahn et al., 2009; Pafundo et al., 2021).

Though some of the available evidence for disrupted gamma in PSZ is drawn from perceptual and cognitive paradigms in which gamma is elicited by task demands (e.g., Cho et al., 2006), a plurality of the literature involves the use of steady-state paradigms to measure the entrained gamma response. In these studies, simple auditory or visual stimuli (such as clicks or flashes) are rapidly presented at a fixed rate (e.g., 40 Hz) while EEG is recorded. G*amma entrainment* is operationalized as the magnitude or coherence of the gamma oscillation evoked at the stimulation frequency. In contrast to gamma elicited by cognitive tasks, which may reflect more naturalistic engagement of neural dynamics but suffers from low signal-to-noise ratio (see Muthukumaraswamy, 2013), the steady-state response (SSR) paradigm consistently elicits a robust gamma oscillatory response that can easily be separated from background noise. Furthermore, recent computational modeling has linked basket cell PV+ interneuron subtype activity with gamma-band SSR, thereby lending support for the use of this paradigm to understand E-I disruption in PSZ (Metzner et al., 2019).

In PSZ, robust gamma entrainment impairments can be observed (e.g., Hirano et al., 2015; Krishnan et al., 2009; Kwon et al., 1999; Light et al., 2006; Spencer et al., 2008; J. Wang et al., 2018), which is interpreted as a corroboration of the post-mortem literature showing significant disruptions in PV+ interneuron activity (see Tada et al., 2020 for a review; see also Metzner et al., 2019). Indeed, a meta-analysis of auditory SSR studies found that 40 Hz entrainment in PSZ is reduced in both amplitude and intertrial phase coherence, with effect sizes (Cohen's *d*) of 0.58 and 0.46, respectively (Thuné et al., 2016). Taken together, auditory gamma entrainment appears to mirror the pattern of PV+ interneuron disruption in PSZ and is thought to reflect the physiological mechanism by which cognition is impacted in this patient population.

Despite this complementary pattern of results linking the postmortem and *in vivo* electrophysiology literature, some conceptual gaps remain. First, nearly all of the gamma entrainment literature in PSZ is limited by its exclusive focus on the auditory pathway. One reason for this historical trend is that the cytoarchitecture of the primary auditory cortex is such that it tends to preferentially oscillate at gamma frequencies. Galambos and colleagues (1981) observed that it entrains most readily to 40 Hz stimulation, and less robustly to slower stimulation rates such as 20 or 30 Hz. By contrast, the visual cortex tends to preferentially oscillate at frequencies in the alpha range (9-13 Hz). Though these physiological differences between primary sensory cortices are widely known, the link between PV+ interneuron disruption and gamma production capacity should theoretically remain the same, irrespective of brain region. That is, although gamma is not the dominant frequency in visual cortex, there is no reason to suspect that gamma-band entrainment is any less dependent upon PV+ interneurons in the visual cortex than in the auditory cortex.

Furthermore, given the ubiquitous nature of PV+ interneuron disruption from the prefrontal (Kaar et al., 2019) to the occipital cortex (Fish et al., 2021), it might be expected that gamma entrainment abnormalities should be observable across sensory modalities, especially if

these abnormalities relate to the broad spectrum of cognitive deficits in PSZ. Note that it is not necessarily assumed that the magnitude of impairment is equal across sensory modalities; it is only assumed that gamma entrainment abnormalities should be observed to some degree in cortical regions characterized by PV+ interneuron disruption. To date, however, few studies have examined this possibility in PSZ. In these rare cases, the results have been mixed: Krishnan and colleagues (2005) found that occipital gamma entrainment to a visual flicker stimulus was reduced in PSZ relative to HCS, whereas Murphy & Dost (2019) observed no significant differences in visual gamma entrainment between first episode PSZ and HCS. It is therefore currently unclear the degree to which gamma entrainment abnormalities in PSZ represent a unitary, cortex-wide phenomenon mirroring the PV+ interneuron disruption observed in the postmortem literature.

A second significant gap in the literature concerns the relationship between entrained gamma and cognitive functioning in PSZ. The gamma entrainment literature largely rests on the assumption that the oscillatory responses elicited by the SSR paradigm reflect neural circuits that are critical for cognitive function; however, direct evidence that individual differences in gamma entrainment are correlated with behavioral performance is scarce, and inconsistent when reported. Although some studies have reported evidence for the expected association between robust gamma entrainment and higher cognitive functioning in PSZ (e.g., Light et al., 2006), others have found that more gamma entrainment is significantly correlated with *lower* IQ among healthy older adults (Horwitz et al., 2017). Similarly, Kim and colleagues (2019) observed that reduced gamma entrainment among PSZ was significantly associated with *higher* performance on a verbal fluency task. In the largest available study to date (N=234 PSZ), Kirihara and colleagues (2012) found no significant relationship between gamma entrainment and verbal memory, executive function, or auditory working memory. Thus, despite the conceptual thread linking gamma oscillations to cognition, and despite the computational modeling linking PV+ interneuron disruption to SSR abnormalities in PSZ, it remains unclear whether gamma entrainment elicited by the SSR paradigm constitutes a meaningful assay of cortex-wide microcircuitry disruption that is associated with cognitive impairment in PSZ.

The present study had two primary goals. First, we tested the hypothesis that gamma entrainment abnormalities can be observed in PSZ across sensory modalities, and the related hypothesis that the gamma-band SSR activity would be correlated across modalities in PSZ. Such findings would support the assumption that the SSR taps into a common microcircuitry impairment throughout the cortex. Second, we tested the hypothesis that individual and group differences in cross-modal gamma entrainment reflect variation in biological processes associated with cognitive functioning. Though there is some evidence that *endogenous* gamma elicited by tasks engaging cognitive processes such as executive control and working memory is associated with successful performance of these tasks (Cho et al., 2006; Kang, 2018; Singh et al., 2020), it is less clear that SSR-evoked gamma entrainment reflects the same core physiological process necessary for cognitive function.

To achieve these aims, we measured entrainment at 20, 30, and 40 Hz in the auditory and visual modalities in a relatively large sample of PSZ and HCS (total N=158). These stimulation rates were selected to assess entrainment in two gamma frequencies (30 and 40

Hz), as well as within the beta frequency band (20 Hz), which is not typically presumed to emerge from cortical PV+ interneuron modulation. We predicted that entrainment to gamma frequencies would be disrupted in PSZ, and that the magnitude of that disruption would be associated across modalities. Furthermore, we predicted that gamma-band entrainment but not beta-band entrainment would be associated with cognitive performance.

Methods

Participants

The present study included 78 individuals meeting DSM-IV-TR criteria for schizophrenia or schizoaffective disorder and 80 psychiatrically healthy individuals (Table 1). The groups were similar with respect to age, sex, race, and parental education, a proxy measure of socioeconomic status. The groups differed significantly on IQ and educational attainment. Diagnosis was established using the Structured Clinical Interview for the DSM-IV (First et al., 2015) by trained, masters-level research staff and review of medical records and informant reports when appropriate. All PSZ were clinically stable with no medication changes for at least 4 weeks. HCS had no current Axis I diagnosis or schizotypal personality disorder, were not taking psychiatric medications, and reported no family history of psychosis. All participants were 18-55 years old, reported no history of neurologic injury, and were free from a substance use disorder in the 6 months prior to testing. PSZ were recruited from the Maryland Psychiatric Research Center and other community clinics, whereas HCS were recruited from the local community by advertisement. All recruiting methods and experimental procedures were approved by the University of Maryland Institutional Review Board.

Neuropsychological and Symptom Measures

The following neuropsychological measures were administered: The MATRICS Consensus Cognitive Battery (MCCB; Nuechterlein et al., 2008), the Wide Range Achievement Test (WRAT; Wilkinson & Robertson, 2006), the Wechsler Test of Adult Reading (WTAR; Wechsler, 2001), and the Wechsler Abbreviated Scale of Intelligence (WASI; Wechsler, 2011). Additionally, visual working memory was assessed using a 4-item change localization task (see Gold et al., 2019 for details). Current symptom severity level was measured by trained and calibrated raters using the Brief Psychiatric Rating Scale (Overall & Gorham, 1962) and the Scale for the Assessment of Negative Symptoms (Andreasen, 1989). Finally, social and occupational functioning was assessed using the total value of these two subscales from the Level of Functioning Scale (Schneider & Struening, 1983).

Experimental Paradigm and Apparatus

In the auditory condition, click trains were administered binaurally via Etymotic earphone inserts (Etymotic Research, Inc., Elk Grove Village, IL) while participants sat in a relaxed but alert state and fixated a cross at a nominal viewing distance of 100 cm. Click trains were 500 ms in duration with an onset-to-onset interval of 1000 ms, and were delivered at 20, 30, and 40 Hz stimulation rates. In the visual condition, stimuli consisted of 20, 30, and 40 Hz white flashes delivered through a custom light-emitting diode panel placed at a nominal viewing distance of 100 cm. As with the auditory stimuli, the flash trains were 500

ms in duration with an ITI of 1000 ms. Both auditory and visual stimuli were presented using Psychtoolbox 3.0 (Brainard, 1997; Kleiner et al., 2007; Pelli, 1997) in MATLAB (The MathWorks, Inc., Natick, MA). Participants received 175 trains of each stimulation rate for each modality, divided into 5 blocks of trials for each modality, with stimulation rate varying randomly within each block. All 5 blocks for a given modality were presented consecutively, and the order of modalities was counterbalanced across participants.

Electroencephalogram Recording and Analysis

The EEG was recorded from two different active electrode systems over the course of the study: (1) a 39-channel BioSemi ActiveTwo system at 2048 Hz with a fifth-order sinc antialiasing filter (half-power cutoff at 416 Hz) (BioSemi B.V., Amsterdam, Netherlands); and (2) a 64-channel Brain Products ActiCHamp system at 5000 Hz with a cascaded integrator–comb antialiasing filter (half-power cutoff at 1300 Hz). 34 HCS and 43 PSZ were assessed using the BioSemi system, and 46 HCS and 35 PSZ were assessed using the Brain Products system. To standardize recordings across systems, the following steps were taken: first, all data were downsampled to 1000 Hz with a two-way least-squares antialiasing filter with an edge frequency of 450 Hz. Second, data from 30 electrode locations common to both recording montages were extracted: Fp1/Fp2, F7/F8, F3/F4, Fz, FCz, C3/C4, Cz, P9/P10, P7/P8, P5/P6, P3/P4, P1/P2, Pz, PO7/PO8, PO3/PO4, POz, O1/O2, and Oz. Finally, all data from both systems were referenced to the average of P9 and P10 (comparable to averaged mastoids). All further pre-processing and analysis steps were performed on these standardized data sets.

All data processing was conducted in MATLAB using EEGLAB (Delorme & Makeig, 2004) and ERPLAB (Lopez-Calderon & Luck, 2014). EEG data were first high-pass filtered at 0.05 Hz and then segmented from −500 to 1000 ms relative to stimulus train onset and baseline adjusted to the 500 ms pre-train period. Visual inspection was used to identify channels for interpolation and bad epochs for removal. Epochs containing an eye blink during the stimulation period in the visual condition were deleted. Subsequently, independent component analysis was performed to correct for remaining eye movements and blinks. Next, epochs containing large noise (amplitudes that exceeded ±150 μV within a 200-ms moving window) were removed. Finally, the data were visually inspected for any remaining artifacts. All participants retained a minimum of 40% of their data epochs. HCS and PSZ retained 86% and 83% of their trials in the auditory condition, respectively (t_{156}=1.85; p=0.07), and 76% and 70% of their trials in the visual condition, respectively (t_{156}=2.90; p<0.01). To eliminate the possibility that the effects were biased by between-group differences in trial number, a supplementary analysis was performed on a subset of trials that were held constant across participants. The pattern of results remained the same (see Supplementary Materials, Table S1).

Time-Frequency Analysis

Entrainment was calculated in three ways: (1) single-trial event-related spectral perturbation (ERSP), which indicates average event-related change in total signal amplitude (evoked and induced) across trials; (2) inter-trial coherence (ITC), which indicates phase consistency from trial to trial; and (3) phase-lag angle (PLA), which indicates the phase delay of the

oscillatory signal compared to the total sample. These measures capture the magnitude, consistency, and timing of the entrainment response, respectively.

To measure ERSP, a Hanning-tapered three-cycle Morlet wavelet was convolved with the EEG from each channel in 1-Hz steps from 10 Hz to 80 Hz. Power in each frequency band was then baseline adjusted by calculating the proportional change in signal relative to the 500 ms preceding the onset of the stimulus train on a logarithmic scale (dB). Average power was calculated for 100-500 ms after the onset of the stimulus train within the 19-21 Hz, 29-31 Hz, and 39-41 Hz frequency bands for the 20-, 30-, and 40 Hz stimulation rates, respectively.

ITC was similarly calculated for all frequencies between 10 and 80 Hz in 1-Hz steps, using methodology described by Delorme and Makeig (2004). ITC for each stimulation condition and modality was measured using the same time and frequency windows as for the ERSP calculations described above. ITC values range between 0 (no coherence) and 1 (perfect coherence).

To calculate PLA, the phase angle for each bin was extracted from the time-frequency transformation described above, and a grand average of phase angles was calculated using the *circ_mean()* function within the Matlab Circular Statistics Toolbox (Berens, 2009). Individuals' PLA was then calculated by determining the distance (in radians) between each participant's phase angles within the stimulation frequency bins and the grand average of phase angles from all other subjects (N=157; for a detailed explanation of this technique, see Roach et al., 2019). For all three indices, entrainment was measured between 100-500 ms after stimulus train onset at the sites where signals were maximal for both HCS and PSZ (FCz for the auditory modality and Oz for the visual modality).

Data Analysis

In order to contextualize the present results within the broader literature on SSR abnormalities in PSZ, group differences in the three entrainment indices were first examined separately by modality. Specifically, repeated-measures ANOVAs were conducted to examine group differences in ERSP and ITC, whereas a circular statistics toolbox (Berens, 2009) was used to measure group differences in PLA. We next assessed the degree to which entrainment was consistent across modalities using three statistical approaches: first, we examined the correlations between modalities for all entrainment indices; second, we conducted two 3-way ANOVAs (stimulation rate x group x modality), separately for ERSP and ITC entrainment indices; and third, we conducted a principal components analysis (PCA) to examine the degree to which cross-modal entrainment could be accounted for by a common factor. Finally, Spearman correlation coefficients were calculated to examine the relationship between factor scores and measures of cognition and symptom severity, whereas circular correlation coefficients were calculated to examine these same relationships with the PLA entrainment index.

Transparency and Openness

All data, analysis code, and research materials will be made available upon request by emailing the corresponding author. Data were analyzed using Matlab version 2020b. This study's design and its analysis were not pre-registered.

Results

Auditory Entrainment Between Groups

All three measures of auditory entrainment at 40 Hz are depicted in Figure 1; entrainment at 20 Hz and 30 Hz is depicted in Supplementary Figures S1 and S2, respectively. The raw ERSP and ITC averages for each group are depicted in Supplementary Figure S3. ANOVAs (group x stimulation rate) were conducted separately for the ERSP and ITC measures of entrainment. Values from the primary statistical analyses are provided in Table 2.

The ERSP measure exhibited a main effect of stimulation rate, with the largest entrainment response at 40 Hz and the smallest at 20 Hz. This effect is obscured by z-transformed normalization in Figure 1 but can be seen in the non-normalized data shown in Figure S3. There was no main effect of diagnosis, but there was a significant diagnosis x stimulation rate interaction. Follow-up t-tests revealed that PSZ exhibited significantly greater power in the 30 Hz condition (t_{156}=2.87; p<0.01; Cohen's d=0.46 [95% CI = 0.05–0.68]), with no significant group differences in the 20 Hz (t_{156}=0.10; p=0.92; Cohen's d=0.02 [95% CI = −0.29–0.33]) and a trend-level reduction in the PSZ group in the 40 Hz condition (t_{156}=1.85; p=0.07; Cohen's d=0.29 [95% CI = 0.00–0.62]; Figure 1A-1B; interaction depicted in Figure 1C addressed below).

The ITC measure exhibited a similar pattern: a main effect of stimulation rate was observed, with coherence largest at 40 Hz and smallest at 20 Hz (see Figure S3). There was no main effect of diagnosis, but there was again a significant diagnosis x stimulation rate interaction. Follow-up t-tests revealed a significant reduction in coherence in PSZ relative to HCS at the 40 Hz stimulation rate (t_{156}=2.28; p=0.02; Cohen's d=0.36 [95% CI = 0.04–0.67]; Figure 1D-1E; interaction depicted in Figure 1F addressed below), with no significant group differences at the 20 Hz (t_{156}=1.36; p=0.18; Cohen's d=0.22 [95% CI = −0.09–0.53]) or 30 Hz stimulation rates (t_{156}=0.62; p=0.54; Cohen's d=0.10 [95% CI = −0.21–0.41]).

Because phase is a nonlinear measure, group differences in PLA were analyzed using the Matlab Circular Statistics Toolbox (Berens, 2009). Circular means were compared using the Watson-Williams test separately for each stimulation rate, which is analogous to a one-way ANOVA (Mardia & Jupp, 2000). We observed that PSZ significantly lagged HCS in the 40-Hz condition (Figure 1G-1H; for a visualization see Figure 1I) and lagged HCS in the 30-Hz condition at the trend level, but did not differ from HCS in the 20 Hz condition.

40 Hz entrainment demonstrated excellent internal consistency for all three measures (split-half reliability > 0.93; Supplementary Table S2). In the 30 Hz stimulation condition, excellent internal consistency was achieved for the ITC and PLA measures (split-half reliability > 0.90), but only moderate internal consistency for the ERSP measure (0.64-0.70).

By contrast, the entrainment response in the 20 Hz condition demonstrated poor-to-moderate internal consistency (split-half reliability = 0.36-0.88).

Visual Entrainment Between Groups

All three measures of visual entrainment at 40 Hz are depicted in Figure 2; entrainment at 20 and 30 Hz is depicted in Supplementary Figures S4 and S5, respectively. The raw ERSP and ITC averages for each group are depicted in Supplementary Figure S3. ANOVAs (group x stimulation rate) were conducted separately for the ERSP and ITC measures of entrainment (see Table 2 for statistics).

For the ERSP measure, there was a main effect of stimulation rate (Figure S3). Specifically, entrainment was significantly smaller in the 40 Hz condition compared to the 20- and 30 Hz conditions (t's>5.13; p's<0.001), which were not significantly different from one another (t_{157}=0.89; p=0.38). As shown in Figure 2, there was also a main effect of diagnosis, with PSZ exhibiting reduced entrainment at all three stimulation rates (20 Hz: t_{156}=2.60; p=0.01; Cohen's d=0.41 [95% CI = 0.09–0.72]; 30 Hz: t_{156}=3.48; p=0.001; Cohen's d=0.55 [95% CI = 0.23–0.87]; 40 Hz: t_{156}=3.31; p=0.001; Cohen's d=0.53 [95% CI = 0.21–0.84]; Figure 2A-2B; interaction depicted in Figure 2C addressed below). There was no significant diagnosis x stimulation rate interaction (p=0.36).

The ITC measure exhibited a similar pattern, with a main effect of stimulation rate driven by reduced entrainment in the 40 Hz condition compared to both the 20- and 30 Hz conditions (t's>3.51; p's<0.001), which were not significantly different from one another (t_{157}=0.18; p=0.86). There was a significant main effect of diagnosis and a trend-level diagnosis x stimulation rate interaction; follow-up t-tests revealed that whereas PSZ exhibited significantly reduced entrainment relative to HCS at all three stimulation rates, this reduction was larger in the 30- and 40 Hz conditions (t's>4.12; p's<0.001; Cohen's d's=0.66 [95% CI = 0.34–0.98]; Figure 2D-2E; interaction depicted in Figure 2F addressed below) than for the 20 Hz condition (t_{156}=2.32; p<0.05; Cohen's d=0.37 [95% CI = 0.05–0.68]).

As with the auditory condition, the Watson-Williams test was used to measure group differences in PLA. In the 20 Hz condition, PSZ significantly *led* the HCS entrainment response; by contrast, PSZ *lagged* HCS at a trend level in the 40 Hz condition (p=0.09; Figure 2G-2H; for a visualization see Figure 2I).

All entrainment measures demonstrated excellent internal consistency for all visual stimulation rates (all split-half reliability indices > 0.88; Supplementary Table S2).

Correlations between modalities

Of central interest is the degree to which abnormalities in the SSR—and gamma entrainment in particular—are correlated across modalities and therefore plausibly reflect a common neural mechanism. Spearman correlations were conducted on ERSP and ITC measures across modality for each stimulation rate, separately by group. Because the PLA measure is in circular space, correlations were calculated using Matlab's circ_corrcc() function. Table 3 depicts cross-modality correlations for each stimulation rate. In PSZ, visual and auditory ERSP and ITC were weakly but significantly correlated at the 40 Hz stimulation

rate. Additionally, visual and auditory ITC exhibited a trend-level correlation at the 20 Hz stimulation rate. No significant correlations were observed for the 30 Hz rate. PLA correlations between modalities were not significant for either group at any stimulation rate. The two groups did not differ significantly from one another in the strength of the correlations in entrainment between modalities for any stimulation rate.

Interaction between diagnosis, modality, and stimulation rate

To further test the hypothesis that a unitary trans-cortical mechanism accounts for SSR abnormalities in PSZ, we entered the auditory and visual data into a 3-way ANOVA (diagnosis x modality x stimulation rate) after applying a z transformation to normalize the data within each modality. By normalizing the data, we eliminated the influence of the modality x stimulation rate interaction, which is profound and is a consequence of known anatomical and functional connectivity differences across the two sensory pathways. Because the PLA measure is in circular space, this index was not included in the analysis. The z-transformed ERSP and ITC values for all stimulation rates are depicted in Figure 1C and 1F (auditory), and Figure 2C and 2F (visual). The ANOVA yielded a main effect of diagnosis for both ERSP ($F_{1,156}=5.34$; $p=0.02$; $\eta^2_p=0.03$) and ITC ($F_{1,156}=14.33$; $p<0.001$; $\eta^2_p=0.08$), indicating a pattern of reduced entrainment in PSZ. Due to the normalization step, main effects of modality, stimulation rate, and interactions between modality and stimulation rate were necessarily null (all F's=0.00; all p's=1.00).

Importantly, and of central interest to the study, we observed a significant 3-way interaction between diagnosis, modality, and stimulation rate for both ERSP ($F_{1.87,291.10}=5.83$; $p<0.01$; $\eta^2_p=0.04$) and ITC ($F_{1.88,293.37}=3.71$; $p=<0.05$; $\eta^2_p=0.02$). This 3-way interaction indicates that the pattern of group differences across stimulation rate significantly differs between the two modalities. This observation dovetails with the above finding of low cross-modality correlations in entrainment. Both the correlations and the ANOVA indicate that gamma-band entrainment is largely modality-specific.

Correlations with measures of cognition and symptom severity

Because of the large number of measures, we reduced the dimensionality of the data using a principal component analysis (PCA) on the two z-transformed entrainment indices (ERSP, ITC) at all stimulation rates. Correlations between PLA and cognition were examined separately. Three components were extracted based on an eigenvalue threshold of 1.0; factor loadings for each of the entrainment measures can be found in Supplementary Table S3. Visual entrainment at all three stimulation rates loaded onto component 1. Auditory entrainment was captured by components 2 and 3, with 30- and 40 Hz entrainment measures loading onto component 2 and 20 Hz entrainment measures loading onto component 3. These loadings are again consistent with the hypothesis of a common source of variance within modality and little shared variance across modalities. The three component scores were then correlated with measures of cognition, separately for HCS and PSZ. Associations between cognition and PLA indices were assessed using Matlab's circ corrcl() function, which is designed to measure correlations between circular and linear data.

Correlations between component scores, cognition, and clinical measures can be found in Supplementary Table S4. In HCS, we observed a significant relationship between auditory gamma entrainment and overall cognition as measured by the WASI, WRAT, and WTAR. Of the MCCB domains, auditory gamma entrainment was significantly correlated with working memory. No such significant correlations were observed between auditory gamma entrainment and any clinical or cognitive measures for PSZ. Neither group exhibited any significant correlations for visual entrainment or for 20 Hz auditory entrainment, with the exception of a small but significant correlation between visual entrainment and WTAR among HCS.

Correlations between PLA and cognitive and clinical measures can be found in Supplementary Tables S5 and S6. PLA exhibited an inconsistent association with clinical and cognitive measures. For example, auditory 40 Hz PLA was significantly associated with WTAR in both HCS and PSZ; however, this relationship was positive for PSZ (i.e., leading the grand average was associated with higher WTAR scores), and negative for HCS (i.e., leading the grand average was associated with lower WTAR scores). No consistent pattern in the relationship between PLA and cognition or symptom severity was observed for either HCS or PSZ, in either the auditory or visual modality. Of note, the strength of the correlations between entrainment and clinical and cognitive variables did not differ significantly between the two groups for any stimulation rate, or for any entrainment index (all p's>0.05).

Discussion

In the present study, we tested two central hypotheses: (1) gamma entrainment is correlated across modalities, indicating that SSR entrainment abnormalities reveal a transcortical biological deficit in PSZ, and (2) gamma entrainment deficits are linked with impaired cognitive functioning in PSZ. We tested the first hypothesis using three different analytical approaches; in all three analyses, we found little evidence for cross-modality consistency in gamma entrainment.

First, we found that entrainment was poorly correlated across modalities at all three stimulation rates, despite good-to-excellent reliability for most measures. The exception was a modest but statistically significant correlation between modalities at 40 Hz in PSZ, which constitutes some evidence that the local recurrent feedback loops thought to underlie gamma oscillations are disrupted in PSZ in a cortex-wide manner. Second, the visual and auditory entrainment measures loaded onto separate components in a PCA. If gamma entrainment varies across individuals as a result of variations in a shared physiological process, we would have expected to find a component with high loadings for both the auditory and visual 40 Hz conditions. Finally, auditory and visual stimuli produced completely different patterns of effects in PSZ and HCS, as evidenced by a 3-way interaction between diagnosis, modality, and stimulation rate in the ERSP and ITC measures. Specifically, whereas PSZ exhibited attenuated entrainment at all three stimulation rates in the visual modality, PSZ exhibited abnormally *enhanced* entrainment at 30 Hz in the auditory modality and modest or nonsignificant impairments at 20 Hz and 40 Hz. Thus, although we expected to find

that gamma entrainment abnormalities in PSZ reflect a single, trans-cortical neurobiological process, we found little support for this hypothesis.

We next tested the hypothesis that gamma entrainment is associated with cognitive function and clinical symptom severity. Surprisingly, we found that entrainment was correlated with cognition mainly in HCS and was largely limited to auditory gamma. We found only weak and sporadic correlations in PSZ. Together, these results suggest that gamma oscillations elicited by repetitive stimulus trains do not reflect a unitary neural process that differentiates individuals along the spectrum of cognitive function.

At first glance, these findings appear to contradict reports that gamma is associated with perception (Spencer et al., 2004; Tallon-Baudry & Bertrand, 1999; Wynn et al., 2015) and cognition (Giraud et al., 2007; Sauseng et al., 2009) during experimental tasks. One possible explanation for these seemingly contradictory observations is that entrained gamma oscillations may not reflect the same neural mechanisms that give rise to the endogenous gamma that supports cognitive and perceptual processes. Indeed, recent work using magnetoencephalography has indicated that endogenous gamma and gamma driven by photic stimulation can coexist and emerge from different neural populations within the visual cortex (Duecker et al., 2021). The available evidence thus suggests that evoked gamma by way of the SSR paradigm may not constitute the most powerful assay of microcircuitry disruption linked to sensory and cognitive impairment in PSZ.

There are some differences between the present study and the broader literature. Our finding that 40 Hz auditory entrainment was minimally reduced in PSZ relative to HCS is somewhat at odds with a meta-analytic report that power and phase locking at 40 Hz are impaired in this population, with an effect size (Cohen's d) of 0.58 and 0.46, respectively (Thuné et al., 2016). We found that PSZ exhibited reduced auditory ERSP and ITC at 40 Hz at effect sizes of 0.29 and 0.36, respectively, which was not large enough to rise to the level of statistical significance for the ERSP index. Although the effect sizes observed in the present analysis are somewhat lower than those estimated from the meta-analysis, they are similar to other larger-N studies in which auditory 40 Hz entrainment effect sizes were estimated to be 0.30-0.35 (Kirihara et al., 2012; Rass et al., 2012). By contrast, we found that visual entrainment was impaired in PSZ across all three stimulation rates (Cohen's d's: 0.37-0.66), which replicates previous reports of impaired visual entrainment in the beta and gamma frequency ranges (Krishnan et al., 2005). Thus, there is little reason to believe that our sample of PSZ was unusual. It is important to note, however, that all PSZ were receiving antipsychotic medications at the time of testing; although entrainment measures were uncorrelated with dosage, the potentially normalizing influences of medication cannot be ruled out at this time. Finally, it is important to note that only the lower range of gamma frequencies was assessed, due in part to practical constraints in stimulating the visual cortex at higher frequencies. The possibility that cognition exhibits a relationship to gamma entrainment at higher frequencies therefore can also not be ruled out at this time.

The present data indicate that although PSZ exhibit altered entrainment in beta and gamma, the pattern of impairment varies across modalities and cortical regions. Furthermore, evoked beta and gamma were minimally correlated with cognitive, symptom, and functional

outcome measures in PSZ. To the extent that entrainment reflects the integrity of cortical E-I, these results suggest that E-I disruptions among PSZ may be regionally specific rather than reflecting a cortex-wide microcircuitry impairment. Furthermore, alongside other recent work (Duecker et al., 2021), the present results suggest that gamma-band entrainment protocols are suboptimal for measuring individual differences in cortical function that account for cognitive variation within healthy and psychiatrically ill populations.

Supplementary Material

Refer to Web version on PubMed Central for supplementary material.

Acknowledgments

References

Andreasen NC (1989). The Scale for the Assessment of Negative Symptoms (SANS): Conceptual and theoretical foundations. The British Journal of Psychiatry. Supplement, 7, 49–58.

Bartley XAF, Lucas XEK, Brady XLJ, Li XQ, Hablitz XJJ, Cowell XRM, & Dobrunz XLE (2015). Interneuron Transcriptional Dysregulation Causes Frequency-Dependent Alterations in the Balance of Inhibition and Excitation in Hippocampus. 35(46), 15276–15290. https://doi.org/DOI:10.1523/JNEUROSCI.1834-15.2015

Bartos M, Vida I, & Jonas P (2007). Synaptic mechanisms of synchronized gamma oscillations in inhibitory interneuron networks. 12.

Berens P (2009). CircStat: A MATLAB Toolbox for Circular Statistics. Journal of Statistical Software, 31(10), 1–21.

Bitanihirwe BKY, & Woo T-UW (2014). Transcriptional dysregulation of γ-aminobutyric acid transporter in parvalbumin-containing inhibitory neurons in the prefrontal cortex in schizophrenia. Psychiatry Research, 220, 1155–1159. 10.1016/j.psychres.2014.09.016 [PubMed: 25312391]

Brainard D (1997). The Psychophysics Toolbox. Spatial Vision, 10, 433–436. [PubMed: 9176952]

Cardin JA (2016). Snapshots of the Brain in Action: Local Circuit Operations through the Lens of 𝒢 Oscillations. 36(41), 10496–10504. https://doi.Org/DOI:10.1523/JNEUROSCI.1021-16.2016

Cho RY, Konecky RO, & Carter CS (2006). Impairments in frontal cortical synchrony and cognitive control in schizophrenia. Proceedings of the National Academy of Sciences, 103(52), 19878–19883. 10.1073/pnas.0609440103

Chung DW, Fish KN, & Lewis DA (2016). Pathological Basis for Deficient Excitatory Drive to Cortical Parvalbumin Interneurons in Schizophrenia. Am J Psychiatry, 173(11), 1131–1139. [PubMed: 27444795]

Cunningham MO, Hunt J, Middleton S, LeBeau FEN, Gillies MG, Davies CH, Maycox PR, Whittington MA, & Racca C (2006). Region-Specific Reduction in Entorhinal Gamma Oscillations and Parvalbumin-Immunoreactive Neurons in Animal Models of Psychiatric Illness. 26(10), 2767–2776. https://doi.org/DOI:10.1523/JNEUROSCI.5054-05.2006

Danos P, Baumann B, Bernstein HG, Franz M, Stauch R, Northoff G, Krell D, Falkai P, & Bogerts B (1998). Schizophrenia and anteroventral thalamic nucleus: Selective decrease of parvalbumin-immunoreactive thalamocortical projection neurons. Psychiatry Research, 82(1), 1–10. 10.1016/s0925-4927(97)00071-1 [PubMed: 9645546]

Delorme A, & Makeig S (2004). EEGLab: An open source toolbox for analysis of single-trial EEG dynamics including independent component analysis. Journal of Neuroscience, 134, 9–21.

Dricks S (2016). Effects of neonatal stress on gamma oscillations in hippocampus. Scientific Reports, 6, 29007. https://doi.org/DOI: 10.1038/srep29007 [PubMed: 27363787]

Duecker K, Gutteling TP, Herrmann CS, & Jensen O (2021). No Evidence for Entrainment: Endogenous Gamma Oscillations and Rhythmic Flicker Responses Coexist in Visual Cortex. The Journal of Neuroscience, 41(31), 6684–6698. 10.1523/JNEUROSCI.3134-20.2021 [PubMed: 34230106]

First M, Williams J, Karg R, & Spitzer R (2015). Structured Clinical Interview for DSM-5—Research Version (SCID-5 for DSM-5, Research Version; SCID-5-RV). American Psychiatric Association.

Fisahn A, Neddens J, Yan L, & Buonanno A (2009). Neuregulin-1 Modulates Hippocampal Gamma Oscillations: Implications for Schizophrenia. 19, 612–618. https://doi.org/doi:10.1093/cercor/bhn107

Fish KN, Rocco BR, DeDionisio AM, Dienel SJ, Sweet RA, & Lewis DA (2021). Altered Parvalbumin Basket Cell Terminals in the Cortical Visuospatial Working Memory Network in Schizophrenia. 90, 47–57. 10.1016/j.biopsych.2021.02.009

Galambos R, Makeig S, & Talmachoff PJ (1981). A 40-Hz auditory potential recorded from the human scalp. Proceedings of the National Academy of Sciences, 78(4), 2643–2647. 10.1073/pnas.78.4.2643

Giraud A-L, Kleinschmidt A, Poeppel D, Lund TE, Frackowiak RSJ, & Laufs H (2007). Endogenous Cortical Rhythms Determine Cerebral Specialization for Speech Perception and Production. Neuron, 56(6), 1127–1134. 10.1016/j.neuron.2007.09.038 [PubMed: 18093532]

Gold JM, Barch DM, Feuerstahler LM, Carter CS, MacDonald AW, Ragland JD, Silverstein SM, Strauss ME, & Luck SJ (2019). Working Memory Impairment Across Psychotic disorders. Schizophrenia Bulletin, 45(4), 804–812. 10.1093/schbul/sby134 [PubMed: 30260448]

Gonzalez-Burgos G, Cho RY, & Lewis DA (2015). Alterations in Cortical Network Oscillations and Parvalbumin Neurons in Schizophrenia. 77, 1031–1040. 10.1016/j.biopsych.2015.03.010

Hirano Y, Oribe N, Kanba S, Onitsuka T, Nestor PG, & Spencer KM (2015). Spontaneous Gamma Activity in Schizophrenia. JAMA Psychiatry, 72(8), 813. 10.1001/jamapsychiatry.2014.2642 [PubMed: 25587799]

Horwitz A, Dyhr Thomsen M, Wiegand I, Horwitz H, Klemp M, Nikolic M, Rask L, Lauritzen M, & Benedek K (2017). Visual steady state in relation to age and cognitive function. PLOS ONE, 12(2), e0171859. 10.1371/journal.pone.0171859 [PubMed: 28245274]

Joshi D, Catts VS, Olaya JC, & Shannon Weickert C (2015). Relationship between somatostatin and death receptor expression in the orbital frontal cortex in schizophrenia: A postmortem brain mRNA study. Npj Schizophrenia, 1(1), 14004. 10.1038/npjschz.2014.4 [PubMed: 27336026]

Kaar SJ, Angelescu I, Marques TR, & Howes OD (2019). Pre-frontal parvalbumin interneurons in schizophrenia: A meta-analysis of post-mortem studies. 126, 1637–1651. 10.1007/s00702-019-02080-2

Kang SS (2018). Abnormal cortical neural synchrony during working memory in schizophrenia. Clinical Neurophysiology, 12.

Kilonzo VW, Sweet RA, Glausier JR, & Pitts MW (2020). Deficits in Glutamic Acid Decarboxylase 67 Immunoreactivity, Parvalbumin Interneurons, and Perineuronal Nets in the Inferior Colliculus of Subjects With Schizophrenia. Schizophrenia Bulletin, 46(5), 1053–1059. 10.1093/schbul/sbaa082

Kim S, Jang S-K, Kim D-W, Shim M, Kim Y-W, Im C-H, & Lee S-H (2019). Cortical volume and 40-Hz auditory-steady-state responses in patients with schizophrenia and healthy controls. NeuroImage: Clinical, 22, 101732. 10.1016/j.nicl.2019.101732 [PubMed: 30851675]

Kirihara K, Rissling AJ, Swerdlow NR, Braff DL, & Light GA (2012). Hierarchical Organization of Gamma and Theta Oscillatory Dynamics in Schizophrenia. Biological Psychiatry, 71(10), 873–880. 10.1016/j.biopsych.2012.01.016 [PubMed: 22361076]

Kleiner M, Brainard D, & Pelli D (2007). What's new in Psychtoolbox-3? European Conference on Visual Perception.

Knable M, Webster M, Meador-Woodruff J, & Torrey E (2004). Molecular abnormalities of the hippocampus in severe psychiatric illness: Postmortem findings from the Stanley Neuropathology Consortium. Molecular Psychiatry, 9, 609–620. [PubMed: 14708030]

Konradi C, Yang CK, Zimmerman EI, Lohmann KM, Gresch P, Pantazopoulos H, Berretta S, & Heckers S (2011). Hippocampal interneurons are abnormal in schizophrenia. Schizophrenia Research, 131, 165–173. https://doi.org/doi:10.1016/j.schres.2011.06.007 [PubMed: 21745723]

Krishnan GP, Hetrick WP, Brenner CA, Shekhar A, Steffen AN, & O'Donnell BF (2009). Steady state and induced auditory gamma deficits in schizophrenia. NeuroImage, 47(4), 1711–1719. 10.1016/j.neuroimage.2009.03.085 [PubMed: 19371786]

Krishnan GP, Vohs JL, Hetrick WP, Carroll CA, Shekhar A, Bockbrader MA, & O'Donnell BF (2005). Steady state visual evoked potential abnormalities in schizophrenia. Clinical Neurophysiology, 116(3), 614–624. 10.1016/j.clinph.2004.09.016 [PubMed: 15721075]

Kwon JS, O'Donnell BF, Wallenstein GV, Greene RW, Hirayasu Y, Nestor PG, Hasselmo ME, Potts GF, Shenton ME, & McCarley RW (1999). Gamma Frequency-Range Abnormalities to Auditory Stimulation in Schizophrenia. Archives of General Psychiatry, 56(11), 1001. 10.1001/archpsyc.56.11.1001 [PubMed: 10565499]

Lewis DA, Curley AA, Glausier JR, & Volk DW (2012). Cortical parvalbumin interneurons and cognitive dysfunction in schizophrenia. 35(1), 57–67. 10.1038/s41386-021-01089-0

Light GA, Hsu JL, Hsieh MH, Meyer-Gomes K, Sprock J, Swerdlow NR, & Braff DL (2006). Gamma Band Oscillations Reveal Neural Network Cortical Coherence Dysfunction in Schizophrenia Patients. Biological Psychiatry, 60(11), 1231–1240. 10.1016/j.biopsych.2006.03.055 [PubMed: 16893524]

Lopez-Calderon J, & Luck SJ (2014). ERPLAB: An open-source toolbox for the analysis of event-related potentials. Frontiers in Human Neuroscience, 8, 213–214. [PubMed: 24782741]

Mardia K, & Jupp P (2000). Directional Statistics. John Wiley & Sons Ltd.

Metzner C, Zurowski B, & Steuber V (2019). The Role of Parvalbumin-positive Interneurons in Auditory Steady-State Response Deficits in Schizophrenia. 9, 18525. 10.1038/s41598-019-53682-5

Murphy M, & Ongur D (2019). Decreased peak alpha frequency and impaired visual evoked potentials in first episode psychosis. NeuroImage: Clinical, 22, 101693. 10.1016/j.nicl.2019.101693 [PubMed: 30825710]

Muthukumaraswamy SD (2013). High-frequency brain activity and muscle artifacts in MEG/EEG: A review and recommendations. Frontiers in Human Neuroscience, 7. 10.3389/fnhum.2013.00138

Nuechterlein K, Green M, Kern R, Baade L, Barch DM, & Cohen JD (2008). The MATRICS Consensus Cognitive Battery, Part 1: Test Selection, Reliability, and Validity. American Journal of Psychiatry, 165, 203–213. [PubMed: 18172019]

Overall JE, & Gorham DR (1962). The Brief Psychiatric Rating Scale. Psychological Reports, 10, 799–812.

Pafundo DE, Annan CAP, Fulginiti NM, & Belforte JE (2021). Early NMDA Receptor Ablation in Interneurons Causes an Activity-Dependent E/I Imbalance in vivo in Prefrontal Cortex Pyramidal Neurons of a Mouse Model Useful for the Study of Schizophrenia. 1–10. https://doi.org/doi:10.1093/schbul/sbab030

Pelli D (1997). The VideoToolbox software for visual psychophysics: Transforming numbers into movies. Spatial Vision, 10, 437–442. [PubMed: 9176953]

Rass O, Forsyth JK, Krishnan GP, Hetrick WP, Klaunig MJ, Breier A, O'Donnell BF, & Brenner CA (2012). Auditory steady state response in the schizophrenia, first-degree relatives, and schizotypal personality disorder. Schizophrenia Research, 136(1–3), 143–149. 10.1016/j.schres.2012.01.003 [PubMed: 22285558]

Reynolds GP, Beasley CL, & Zhang ZJ (2002). Understanding the neurotransmitter pathology of schizophrenia: Selective deficits of subtypes of cortical GABAergic neurons. 109, 881–889.

Roach BJ, Ford JM, & Mathalon DH (2019). Gamma Band Phase Delay in Schizophrenia. Biological Psychiatry: Cognitive Neuroscience and Neuroimaging, 4(2), 131–139. 10.1016/j.bpsc.2018.08.011 [PubMed: 30314905]

Sauseng P, Klimesch W, Heise KF, Gruber WR, Holz E, Karim AA, Glennon M, Gerloff C, Birbaumer N, & Hummel FC (2009). Brain Oscillatory Substrates of Visual Short-Term Memory Capacity. Current Biology, 19(21), 1846–1852. 10.1016/j.cub.2009.08.062 [PubMed: 19913428]

Schneider LC, & Struening EL (1983). SLOF: a behavioral rating scale for assessing the mentally ill. Social Work Research & Abstracts, 19(3), 9–21. 10.1093/swra/19.3.9 [PubMed: 10264257]

Singh F, Shu I-W, Hsu S-H, Link P, Pineda JA, & Granholm E (2020). Modulation of frontal gamma oscillations improves working memory in schizophrenia. Neuroimage: Clinical, 27, 102339. 10.1016/j.nicl.2020.102339 [PubMed: 32712452]

Smucny J, Dienel SJ, Lewis DA, & Carter CS (2021). Mechanisms underlying dorsolateral prefrontal cortex contributions to cognitive dysfunction in schizophrenia. 17. 10.1038/s41386-021-01089-0

Sohal VS, Zhang F, Yizhar O, & Deisseroth K (2009). Parvalbumin neurons and gamma rhythms enhance cortical circuit performance. Nature, 459(7247), 698–702. 10.1038/nature07991 [PubMed: 19396159]

Spencer KM, Nestor PG, Perlmutter R, Niznikiewicz MA, Klump MC, Frumin M, Shenton ME, & McCarley RW (2004). Neural synchrony indexes disordered perception and cognition in schizophrenia. Proceedings of the National Academy of Sciences, 101(49), 17288–17293. 10.1073/pnas.0406074101

Spencer KM, Salisbury DF, Shenton ME, & McCarley RW (2008). γ-Band Auditory Steady-State Responses Are Impaired in First Episode Psychosis. Biological Psychiatry, 64(5), 369–375. 10.1016/j.biopsych.2008.02.021 [PubMed: 18400208]

Tada M, Kirihara K, Koshiyama D, Fujioka M, Usui K, Uka T, Komatsu M, Kunii N, Araki T, & Kasai K (2020). Gamma-Band Auditory Steady-State Response as a Neurophysiological Marker for Excitation and Inhibition Balance: A Review for Understanding Schizophrenia and Other Neuropsychiatric Disorders. Clinical EEG and Neuroscience, 51(4), 234–243. 10.1177/1550059419868872 [PubMed: 31402699]

Tallon-Baudry C, & Bertrand O (1999). Activity in humans and its role in object representation. Trends in Cognitive Sciences, 3(4), 12.

Thune H, Recasens M, & Uhlhaas PJ (2016). The 40-Hz Auditory Steady-State Response in Patients With Schizophrenia: A Meta-analysis. JAMA Psychiatry, 73(11), 1145. 10.1001/jamapsychiatry.2016.2619 [PubMed: 27732692]

Wang AY, Lohmann KM, Yang CK, Zimmerman EI, Pantazopoulos H, Herring N, Berretta S, Heckers S, & Konradi C (2011). Bipolar disorder type 1 and schizophrenia are accompanied by decreased density of parvalbumin- and somatostatin-positive interneurons in the parahippocampal region. Acta Neuropathologica, 122(5), 615–626. 10.1007/s00401-011-0881-4 [PubMed: 21968533]

Wang J, Tang Y, Curtin A, Chan RCK, Wang Y, Li H, Zhang T, Qian Z, Guo Q, Li Y, Liu X, Tang X, & Wang J (2018). Abnormal auditory-evoked gamma band oscillations in first-episode schizophrenia during both eye open and eye close states. Progress in Neuro-Psychopharmacology and Biological Psychiatry, 86, 279–286. 10.1016/j.pnpbp.2018.04.016 [PubMed: 29705712]

Wechsler D (2001). Wechsler test of adult reading. The Psychological Corporation.

Wechsler D (2011). Wechsler Abbreviated Scale of Intelligence (2nd ed.). NCS Pearson.

Wilkinson G, & Robertson G (2006). WRAT4 Wide Range Achievement Test professional manual (4th ed.). Psychological Assessment Resources, Inc.

Wynn JK, Roach BJ, Lee J, Horan WP, Ford JM, Jimenez AM, & Green MF (2015). EEG Findings of Reduced Neural Synchronization during Visual Integration in Schizophrenia. PLOS ONE, 10(3), e0119849. 10.1371/journal.pone.0119849 [PubMed: 25785939]

Zhang ZJ, & Reynolds GP (2002). A selective decrease in the relative density of parvalbumin-immunoreactive neurons in the hippocampus in schizophrenia. Schizophrenia Research, 55(1–2), 1–10. 10.1016/S0920-9964(01)00188-8 [PubMed: 11955958]
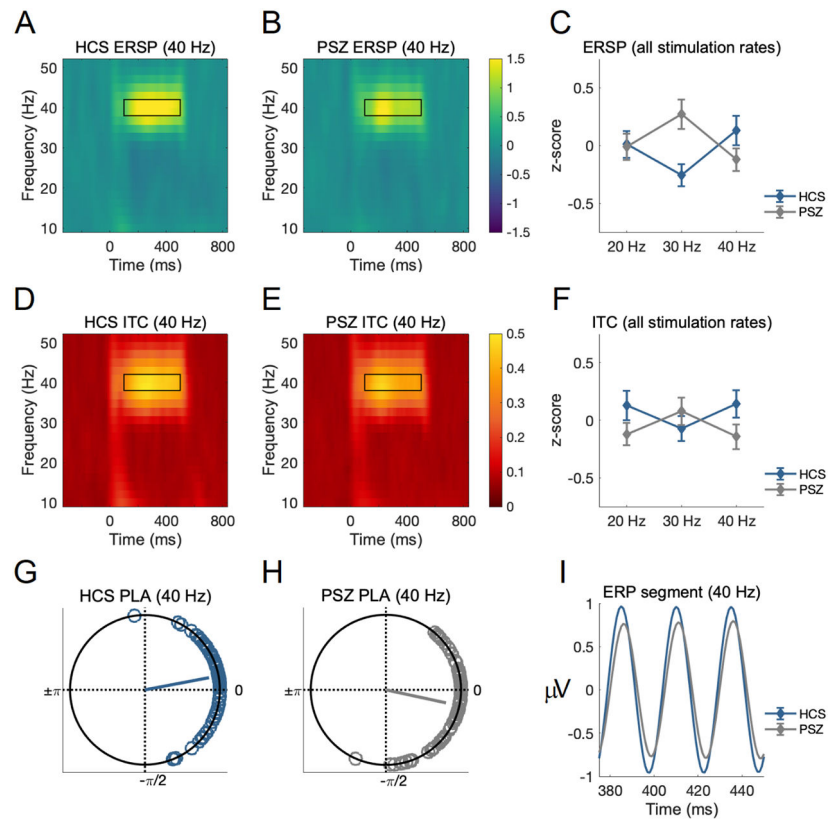
Figure 1.
40-Hz auditory entrainment as measured by ERSP for HCS (A) and PSZ (B); normalized group differences in ERSP entrainment across all three stimulation rates ± SE (C); 40-Hz auditory entrainment as measured by ITC for HCS (D) and PSZ (E); normalized group differences in ITC entrainment across all three stimulation rates ± SE (F); 40-Hz auditory entrainment phase lag for HCS (G) and PSZ (H); grand average ERP segment illustrating phase differences between groups (I).

Figure 2.
40-Hz visual entrainment as measured by ERSP for HCS (A) and PSZ (B); normalized group differences in ERSP entrainment across all three stimulation rates ± SE (C); 40-Hz visual entrainment as measured by ITC for HCS (D) and PSZ (E); normalized group differences in ITC entrainment across all three stimulation rates ± SE (F); 40-Hz visual entrainment phase lag for HCS (G) and PSZ (H); grand average ERP segment illustrating phase differences between groups (I).
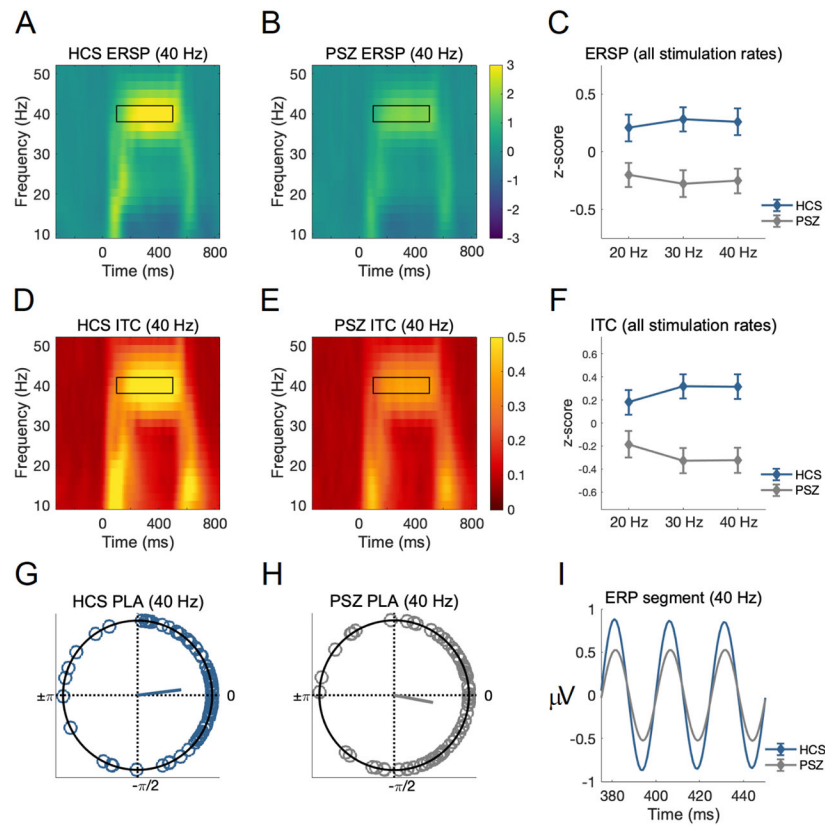
Table 1.

Demographic, cognitive, and clinical variables (mean & SD)

	Healthy Controls	Schizophrenia Patients
Gender (Male : Female)	48 : 32	53 : 25
Age	35.05 (10.48)	37.05 (10.32)
Race (AA : C : Other)	29 : 48 : 3	31 : 43 : 4
Education (years)	15.42 (1.90)	13.30 (2.21) [***]
Parental Education	14.54 (2.41)	13.89 (2.81)
WASI	110.94 (11.65)	97.72 (15.61) [***]
WRAT-4	110.04 (13.86)	98.13 (15.56) [***]
WTAR	112.10 (12.03)	100.11 (17.44) [***]
MATRICS Total	50.67 (9.40)	34.99 (13.10) [***]
MATRICS Processing Speed	52.54 (9.45)	41.41 (12.12) [***]
MATRICS Attention	50.62 (9.56)	41.60 (12.44) [***]
MATRICS Working Memory	51.74 (9.17)	41.48 (10.84) [***]
MATRICS Verbal Learning	50.23 (8.80)	38.40 (8.62) [***]
MATRICS Visual Learning	45.36 (11.28)	37.57 (12.06) [***]
MATRICS Reasoning	50.37 (9.22)	45.67 (10.37) [**]
MATRICS Social Cognition	53.50 (9.40)	40.13 (11.50) [***]
Change Localization	2.91 (0.48)	2.47 (0.65) [***]
BPRS Positive Symptoms	—	2.01 (1.13)
BPRS Negative Symptoms	—	1.67 (0.58)
BPRS Disorganization Symptoms	—	1.17 (0.28)
SANS Total	—	32.47 (8.40)
LOFS Total	—	21.43 (6.10)
Chlorpromazine dose equivalent (mg/day)	—	471.10 (311.75)

[**] $p < 0.01$

[***] $p < 0.001$

AA = African American; C = Caucasian; WASI = Wechsler Abbreviated Scale of Intelligence; WRAT = Wide Range Achievement Test; WTAR = Wechsler Test of Adult Reading; MCCB = MATRICS Consensus Cognitive Battery; BPRS = Brief Psychiatric Rating Scale; SANS = Scale for the Assessment of Negative Symptoms; LOFS = Level of Functioning Scale.

Table 2.

Statistical comparisons for all entrainment measures for both auditory and visual modality, adjusted for nonsphericity using the Huynh-Feldt correction.

	Statistic	df	p	Effect Size	Significant Pairwise Comparisons
Auditory					
ERSP					
Stimulation Rate	F = 218.86	1.44, 223.97	<0.001	$\eta^2_p = 0.58$	20 Hz < 30 Hz < 40 Hz [***]
Diagnosis	F = 0.07	1, 156	0.80	$\eta^2_p = 0.00$	
Stimulation rate x Diagnosis	F = 7.54	1.44, 223.97	<0.01	$\eta^2_p = 0.05$	PSZ > HCS at 30 Hz [**]; HCS > PSZ at 40 Hz [+]
ITC					
Stimulation Rate	F = 341.07	1.80, 280.84	<0.001	$\eta^2_p = 0.69$	20 Hz < 30 Hz < 40 Hz [***]
Diagnosis	F = 2.26	1, 156	0.14	$\eta^2_p = 0.01$	
Stimulation rate x Diagnosis	F = 4.24	1.80, 280.84	0.02	$\eta^2_p = 0.03$	PSZ < HCS at 40 Hz [*]
PLA					
20 Hz Stimulation Rate	F = 0.04	1, 156	0.85	$\eta^2_p = 0.00$	PSZ = HCS
30 Hz Stimulation Rate	F = 3.00	1, 156	0.09	$\eta^2_p = 0.02$	PSZ lagged HCS [+]
40 Hz Stimulation Rate	F = 21.03	1, 156	<0.001	$\eta^2_p = 0.11$	PSZ lagged HCS [***]
Visual					
ERSP					
Stimulation Rate	F = 25.06	1.76, 273.93	<0.001	$\eta^2_p = 0.14$	20 Hz = 30 Hz > 40 Hz [***]
Diagnosis	F = 13.07	1, 156	<0.001	$\eta^2_p = 0.08$	PSZ < HCS at 20 Hz [**]; PSZ < HCS at 30 Hz and 40 Hz [***]
Stimulation rate x Diagnosis	F = 1.00	1.76, 273.93	0.36	$\eta^2_p = 0.01$	
ITC					
Stimulation Rate	F = 10.63	1.72, 268.68	<0.001	$\eta^2_p = 0.06$	20 Hz = 30 Hz > 40 Hz [***]
Diagnosis	F = 16.65	1, 156	<0.001	$\eta^2_p = 0.10$	PSZ < HCS at 20 Hz [*]; PSZ < HCS at 30 Hz and 40 Hz [***]
Stimulation rate x Diagnosis	F = 2.65	1.72, 268.68	0.08	$\eta^2_p = 0.02$	
PLA					
20 Hz Stimulation Rate	F = 6.28	1, 156	<0.05	$\eta^2_p = 0.02$	HCS lagged PSZ [*]
30 Hz Stimulation Rate	F = 2.50	1, 156	0.12	$\eta^2_p = 0.01$	PSZ = HCS

	Statistic	df	p	Effect Size	Significant Pairwise Comparisons
40 Hz Stimulation Rate	F = 2.93	1, 156	0.09	$\eta^2_p = 0.01$	PSZ lagged HCS[+]

[+] p < 0.10

[*] p < 0.05

[**] p < 0.01

[***] p < 0.001

Table 3.

Correlation between auditory and visual modalities for each entrainment measure.

	Healthy Controls	Schizophrenia Patients
ERSP (20 Hz)	0.03	0.18
ERSP (30 Hz)	−0.11	0.07
ERSP (40 Hz)	0.09	0.23 [*]
ITC (20 Hz)	0.17	0.20 [+]
ITC (30 Hz)	−0.05	0.05
ITC (40 Hz)	0.13	0.24 [*]
PLA (20 Hz)	−0.01	0.03
PLA (30 Hz)	−0.16	0.03
PLA (40 Hz)	0.14	0.06

[*]
$p<0.05$